Available free online at www.medjchem.com

Mediterranean Journal of Chemistry **2014**, 3(3), 916-928

Design of Novel Biosensors for Determination of Phenolic Compounds using Catalyst-Loaded Reduced Graphene Oxide Electrodes

Ondrej Kubesa[1,2], Kathleen Morrisey[1], Samantha Mathews[1], John Proetta[1], Christopher Li[1], Petr Skladal[2] and Maria Hepel[1,*]

[1]Department of Chemistry, State University of New York at Potsdam, Potsdam, NY 13676, USA
[2]Department of Biochemistry, Masaryk University, 62500 Brno, Czech Republic

Abstract: Facile and inexpensive method for designing high performance sensors for H_2O_2 and polyphenols has been developed. The proposed sensors are based on high electrocatalytic activity of Prussian Blue (PB) nanoparticles deposited in situ on high surface area graphene nanosheet-based thin films on a graphite electrode. The exfoliated graphene nanosheets were formed by attaching graphene oxide to the electrode surface followed by their electrochemical reduction to obtain the reduced graphene oxide (rGO), providing high surface area and excellent current-carrying capabilities to the sensory film. The PB catalyst nanoparticles were deposited electrochemically on rGO. This procedure is very time efficient as it reduces the time of sensor preparation from 3 days (according to recent literature) to several hours. The proposed method provides simple means to obtain highly reliable and stable sensory films. The sensor shows a dynamic range of 1–500 µM H_2O_2 and a rapid response of 5 s to reach 95% of a steady-state response. When combined with immobilized enzymes (horseradish peroxidase or laccase oxidase), it can serve as a biosensor for polyphenols. As the proof of concept, the response of the enzymatic biosensors to polyphenol catechin has been presented delineating different mechanisms of horseradish peroxidase and laccase operation. The proposed sensors are low cost, reliable, and scalable.

Keywords: biosensor for polyphenols, enzymatic biosensor, hydrogen peroxide sensor, graphene oxide, graphene nanosheet, Prussian Blue electrocatalyst, catechin, horseradish peroxidase, laccase.

Introduction

Graphene nanosheets (GR) and exfoliated graphene oxide (GO) have become new exciting materials for the design of novel devices and sensing platforms in fields spanning from electronics to chemistry and biomedical applications [1-4]. In sensing applications, various forms of GR and GO have been explored, including self-standing GO membranes [5], GR paper [6], carbon quantum dots [7], and others. A variety of sensors based on GR have been constructed, including sensors for dopamine [8,9], glucose [10,11], ascorbic acid [12], NADH [12,13], cancer drugs [14], agents of chemical warfare [15], etc. For some sensors, the hydrophobic interactions of biomolecules with GR are essential, while in other sensors the role of GR is to provide highly efficient current collection/distribution and the extended surface area where a catalyst can be immobilized.

**Corresponding author:Maria Hepel*
E-mail address: hepelmr@potsdam.edu
DOI: http://dx.doi.org/10.13171/mjc.2014.14.06.12

The construction of sensors based on single monolayer GR is very demanding and expensive since it is grown on a substrate surface via chemical vapor deposition (CVD).

Hence, in practice graphene nanosheets are formed in situ using an alternative approach by reduction of exfoliated GO. This reduction leads to a product, reduced graphene oxide (rGO) that exhibits fundamental properties of monolayer graphene but does not have a perfect graphene structure since not all defects created during a GO formation can be repaired during its reduction. Sensors can also be designed with GO, instead of GR. For instance, sensors with GO decorated with Prussian Blue (GO/PB) exhibit good sensitivity toward H_2O_2 [16-18]. However, their cyclic voltammetric (CV) characteristics show high internal film resistance R_f leading to sloped CV appearance. The high R_f contributes to the increased background current and slow sensor response. Graphene oxide can be reduced chemically [19-27] to a converted graphene (rGO), either in solution with hydrazine or sodium borohydride, or in gaseous phase with hydrogen and hydrazine. It has been shown that GO can also be reduced electrochemically in a monolayer GO film [28] and when embedded in an electrodic film [29]. Nevertheless, the reduction of the GO for rGO/PB sensors has mainly been performed by chemical treatment [30].

The purpose of this work has been to design and test new rGO-based sensors for the detection of hydrogen peroxide, H_2O_2. The importance of hydrogen peroxide in living organisms cannot be overestimated as it is one of the main compounds of the group of reactive oxygen species (ROS) which is involved in immune response, cell signaling, and wound healing, but also causes ageing, DNA damage and mutation [31]. Hence, monitoring of H_2O_2 is an important scientific and diagnostic tool. The utilization of the detection of H_2O_2 is also the key element of the basic transduction scheme of many enzyme biosensors [32-34] where the immobilized active oxidases generate H_2O_2 as a byproduct in reactions with analyte biomolecules. To remedy the diminished activity of enzymes due to their surface confinement in a sensory film, a replacement of enzymes with stable electrocatalysts acting as artificial enzymes would offer plausible alternative. The use of electrocatalysts such as Pt, PtRu alloy, cobalt oxide, and others have been proposed. Itaya et al. [35] and others [36] have found that Prussian Blue (PB) in its reduced form (Prussian White, PW) shows an excellent catalytic activity toward reduction of O_2 and H_2O_2. PB, with general formula $Fe_4[Fe(CN)_6]_3$, belongs to the hexacyanometallate family and acts here as the active electron mediator in redox processes. Moreover, it can be deposited on the electrode surface forming a stable film with fairly low solubility in aqueous acidic and neutral solutions[37-40]. Outstanding performance of nanostructured PB catalysts grown on a Pt substrate without overcoat [41] and with poly(azulene) overcoat [42] have been reported.

PB films have previously been deposited on a carbon fiber electrode (CFE) and coated with semi-permeable poly(orthophenylene diamine) polymer enabling sensitive detection of H_2O_2 and discrimination against interferents [43]. Fast scan voltammetric detection of H_2O_2 on unmodified CFE has been reported by Sanford et al. [44] but the analytical signal was only a small fraction of the background current. PB electrodeposited in situ on multi-walled carbon nanotubes has shown high catalytic activity [45]. Furthermore, the PB nanocubes grown on graphene by wet-chemistry method [46] were used for construction of a wide-dynamic range H_2O_2 sensor. Since the exfoliated graphene nanosheets are less expensive than carbon nanotubes and offer higher electric conductance and higher surface area, we have selected rGO as the base material over carbon nanotubes.

In this work, we have investigated the H_2O_2 sensors based on rGO modified with electrodeposited PB nanoparticles. The first attempt to perform electrodeposition of PB on

rGO has recently been reported by Jiang et al.[47]. However, their rGO was obtained in tedious chemical reduction procedure which required wet-chemical reaction with hydrazine, heating to 95 °C, and 3-day dialysis. In order to improve the rGO synthesis, we have applied in this work the electrochemical in situ reduction of GO films, decreasing the time required for synthesis to several minutes. The detection of phenolic compounds using PB-modified sensors with immobilized enzymes has been performed using first-generation sensors with enzyme-modified electrodes[42,48], or second-generation sensors with PB-modified conductive substrates and immobilized enzyme[49]. Recently, the third-generation sensors with PB-mediator and CNT-wired enzyme[49] have been introduced. Wael et al.[50-54] have applied ZnO quantum dots, C_{60} fullerene, and tyrosinase enzyme wired with graphene nanosheets in designing sensors for phenols. In this work, we have employed the rGO/PB-modified graphite third-generation sensors. Phenolic compounds afford antioxidant activity in most plant-derived products. These compounds act as the free radical scavengers, prevent oxidation, and protect cells against oxidative damage. Various enzymes have been used for the design of CFE/PB biosensors for phenols and polyphenols[43], but the activity of these enzymes has been affected by surface confinement. We have constructed nonenzymatic and highly active rGO/PB/ENZ enzymatic biosensors with immobilized enzymes (ENZ) working at a low applied potential in the range -0.2 V to 0.0 V. Different mechanisms of horseradish peroxidase and laccase operation in these biosensors have been elucidated.

Experimental Section

Chemicals

All chemicals were of reagent grade purity and were used without further purification. Graphite flakes (150 µm size), H_2O_2 (30%), and acids were obtained from Sigma-Aldrich Chemical Company (St Louis, MO, U.S.A.). Potassium hexacyanoferrate (III), $K_3[Fe(CN)_6]$, $FeCl_3$ (hydrate), $KMnO_4$, hydrazine, and $NaBH_4$ were purchased from Fisher Scientific Company (Pittsburgh, PA, U.S.A.). Graphite rod of spectroscopic purity (5 mm dia., resistivity 2.9×10^{-4} ohm-in) was obtained from Alfa Aesar (Ward Hill, MA, USA). Glutaraldehyde, catechin, horseradish peroxidase, laccase oxidase were purchased from Sigma-Aldrich. Solutions were prepared using Millipore (Billerica, MA, U.S.A.) Milli-Q deionized water (conductivity σ = 55 nS/cm). They were deoxygenated by bubbling with purified argon.

Apparatus

For voltammetric measurements, a standard electrochemical setup with a potentiostat-galvanostat Model PS-205B from Elchema (Potsdam, NY, U.S.A.) and a Data Logger and Control System, Model DAQ-716v, operating under Voltscan 5.0 data acquisition and processing software (Elchema), was employed. A double-junction Ag/AgCl electrode was used as the reference electrode, a Pt wire as the counter electrode, and a spectroscopic graphite rod (5 mm dia.) sealed to expose only the disk shaped side with geometrical surface area A = 0.196 cm^2 was used as the working electrode. Prior to use, the electrodes were washed in Milli-Q water, polished with alumina slurry, 0.3 µm grain size followed by 0.05 µm grains, to mirror like finish. Electrodes were then dried in Ar flow and activated as described in the Activation procedure, below. All electrode potentials are referred vs. Ag/AgCl (1 M KCl) reference electrode. The Raman spectra were recorded using a Nicolet DXR Raman Microscope (Thermo Fisher Scientific, Waltham, MA, U.S.A.). Raman

measurements were performed in a closed chamber using stabilized 633 nm He-Ne laser with 8 mW power, focused onto a 0.8 μm diameter spot, and measured in the spectral range of 500-3500 cm^{-1}.

Synthesis of graphene oxide

The graphene oxide (GO) was synthesized by a modified Hummers-Marcano method[55,56], based on oxidation of graphite flakes (150 μm size) in a 9:1 mixture of H_2SO_4:H_3PO_4, by adding granular $KMnO_4$ (to final concentration of 6 M). As proposed by Marcano et al. [56], KNO_3 that was used commonly in Hummers-Offeman method[55] has been replaced with increased concentration of $KMnO_4$ to increase the synthesis efficiency and safety. The reaction was maintained at 50 °C for 12 hours under stirring. The slurry was then poured onto ice with addition of H_2O_2 (30%) and sifted through a 300 μm polyester fiber sieve. After filtration, the product in supernatant was ultrasonicated at 40 kHz for 1 hour and then purified by centrifugation (4000 rpm, 4 h) and collected as the solid. Next, the solid was washed consecutively with water, HCl (30%), and ethanol, coagulated with ether and filtered using a 0.45 μm pore size PTFE membrane. The reactions of this procedure do not generate extensive exothermic heat and produce no toxic gases.

Preparation of exfoliated graphene electrodes (SGE/rGO)

Activation of graphite electrode. A spectroscopic graphite electrode (SGE) was washed in deionized water, dried in a N_2 stream and activated in 0.05 M solution of H_2SO_4 by CV from 0.0 to 2.0 V (scan rate 50 mV/s, 8-cycles), washed in deionized water, and dried in N_2 stream.

Formation of GO film. An electrode was immersed into the solution of GO (0.5 mg/mL) for 4 hours. Alternatively, a 35 μL drop of GO solution (0.5 mg/mL) was pipetted onto the electrode surface and dried to form a cast film.

Reduction of GO. Subsequently, a GO film was reduced either by hydrazine, $NaBH_4$, or by electrochemical cathodic treatment. Since the electrochemical reduction has led to the higher activity of the reduced graphene oxide (rGO), this method was selected for further work. After incubation, a GO film was reduced in 0.5 M NaCl solution by CV (0.7 V to -1.1 V vs. Ag/AgCl), as illustrated in Figure 1.

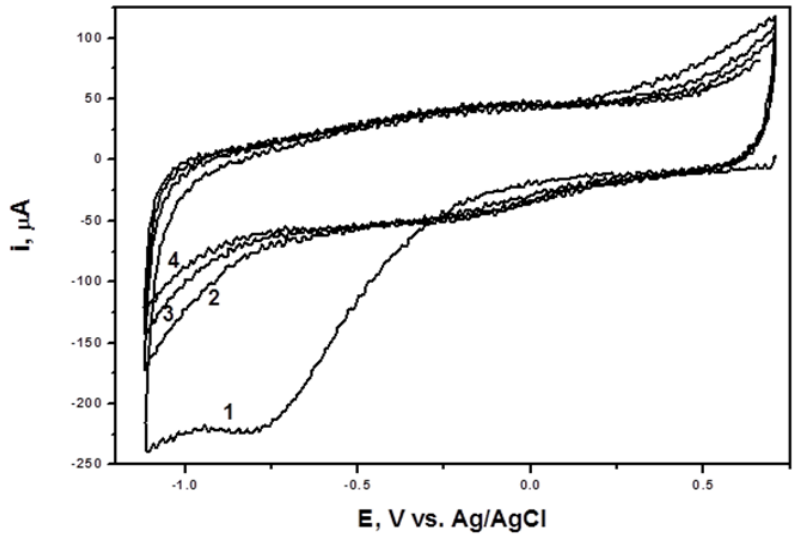

Figure 1. Electrochemical reduction of graphene oxide in 0.5 M NaCl solution; four potential cycles at v = 50 mV/s; electrode surface area: 0.19 cm^2. Most of the reduction occurs during the first cathodic going potential scan. The cycle number is marked at the curves.

It is seen that the GO layer is almost completely reduced during the first scan. The broad GO reduction peak E_p is found at -0,8 V vs. Ag/AgCl. The peak broadness and peak position depend on the composition of GO, as the ratio of various functional groups formed during graphite oxidation (including –OH, aldehyde and ketone >C=O, carboxylate, and epoxide groups) contribute to the GO reduction process. Similar position of the reduction peak (E_p = -0.73 V) for a monolayer oriented GO film in 0.1 M KNO_3, at ν = 10 mV/s has been observed by Ramesha and Sampath[28] in their spectroelectrochemical studies.

The quality of rGO films was monitored using Raman scattering spectroscopy and FTIR. In Figure 2, presented are spectra of different graphene forms showing three main graphene bands: G-band at ν = 1598 cm^{-1}, D-band at ν = 1339 cm^{-1}, and 2D-band at ν = 2687 cm^{-1}. It is seen that in rGO, the 2D band is completely missing since the dual-resonance is inhibited in a graphene lattice containing disorders that cannot be entirely removed by the GO reduction process. The strong G and D bands indicate the presence of perfect graphene domains (G) surrounded by defects (D).

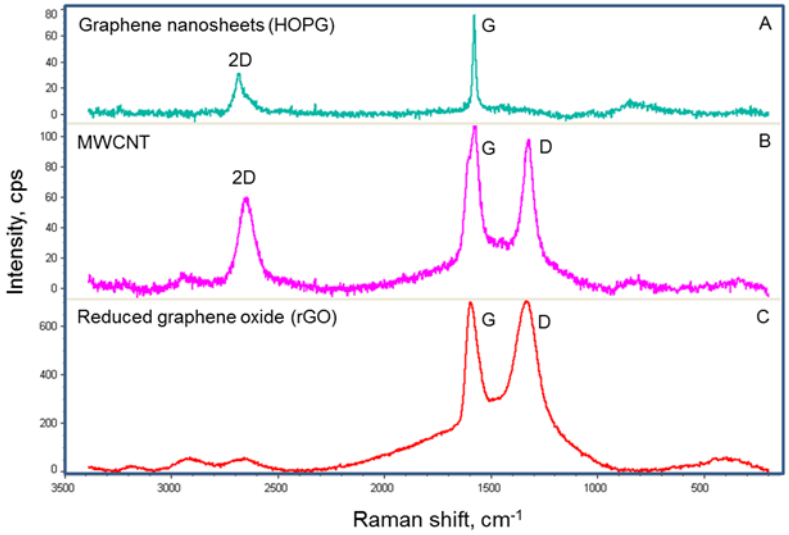

Figure 2. Raman scattering spectra of HOPG graphene multi-nanosheets (A), multi-walled carbon nanotubes (B), and reduced graphene oxide synthesized in this work (C); the bands G, D, and 2D are marked at the respective Raman peaks.

Electrodeposition of Prussian Blue catalyst

The electrolyte bath used for synthesis of supported PB nanoparticle catalyst consisted of a solution of 1.5 mM $K_3[Fe(CN)_6]$ + 1.5 mM $FeCl_3$, containing 0.1 M KCl and 3 mM HCl. The films were deposited using cyclic voltammetry (CV) by applying three scans from -200 mV to 400 mV vs. Ag/AgCl, at scan rate ν = 100 mV/s, in solution deaerated by nitrogen bubbling. After the deposition, films were washed in deionized water, followed by immersion in 0.1 M KCl + 3 mM HCl solution and applying fifty CV scans, using the same protocol. Finally, the PB films were washed in deionized water, dried, and annealed for 2 h at 100 °C and stabilized using the same procedure as for the as-prepared films. The reproducibility of measurements for freshly prepared sensors was 1.4% (n = 8), but decreased by up to ca. 10% after one week when measurements were done in neutral solutions. Better stability was observed in acidic solution, pH 3 to 5. The sensor stability can be further improved by coating sensors with semipermeable polymer membranes but it is out of the scope of the present paper.

Adding enzymes to rGO/PB films

Enzyme films on a SGE/rGO/PB sensor surface were formed by drop casting. The enzyme (horseradish peroxidase or laccase oxidase) was first diluted in a phosphate buffer pH 7.4. Then, an aliquot of BSA (100 mg/mL) was added and solution stirred. Next, gelatin (5 % in water) and glutaraldehyde (2 % solution in water) were added, in ratio 1:10, while stirring the solution. A 20 µL drop of the obtained solution (with enzyme activity 15 U/mg) was immediately pipetted onto the surface of an electrode and left until solvent evaporates. The ready films were then washed with buffer and deionized water and stored under water.

Results and Discussion

Effect of exfoliated rGO on electrocatalytic reduction of H_2O_2

The electrocatalytic activity of bare and rGO-modified graphite electrodes was tested for H_2O_2 reduction in 50 mM PBS buffer, pH 6.0, using linear potential scan voltammetry. In Figure 3, presented are voltammograms obtained in the potential range from E = 0.15 V to E = -0.55 V vs. Ag/AgCl, recorded at the scan rate v = 50 mV/s, for H_2O_2 concentration C_{H2O2} from 0 to 100 mM. The onset of H_2O_2 reduction is observed at E = 0.05 V and the peak potential is: E_p = -0.33 V (at c_{H2O2} = 100 mM; it depends somewhat on H_2O_2 concentration). The dependence of peak current on H_2O_2 concentration (not shown) is linear as expected.

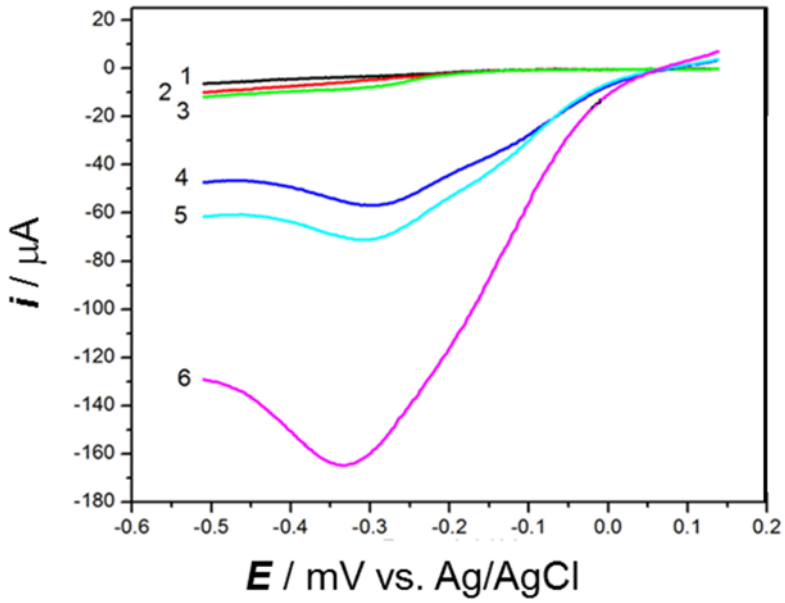

Figure 3. Linear potential scan voltammograms for H_2O_2 reduction on a SGE/Cys/rGO modified electrode in 50 mM PBS buffer, pH 6.0; scan rate v = 50 mV/s.; H_2O_2 concentration, C_{H2O2} [mM]: (1) 0, (2) 1, (3) 5, (4) 25, (5) 50, (6) 100.

The H_2O_2 reduction current at E_p, observed in Figure 3, is high ($|i_p|$ = 165 µA, corresponding to peak current density of 825 µA/cm^2) and thus sensitivity of the electrode toward H_2O_2 is high. However, at high current densities, the analyte depletion occurs quickly in the vicinity of the electrode surface. Therefore, for the purpose of sensing applications, we have limited the cathodic potential to values at the foot of the voltammetric wave. The response of amperometric sensors to H_2O_2, working at a constant potential E = 0 V vs. Ag/AgCl, is analyzed in the following sections. In Figure 4, the dependence of cathodic current on H_2O_2 concentration is presented for SGE and SGE/rGO sensors.

The increase of background current from -0.05 µA to -0.51 µA (extrapolated) is observed. This increase is due to the increased surface area of the electrode and increased double-layer capacitance. The increase of the sensor sensitivity to H_2O_2 is given by:

$$\varepsilon = \frac{\left(\frac{\partial i_2}{\partial c_{H2O2}}\right) - \left(\frac{\partial i_1}{\partial c_{H2O2}}\right)}{\left(\frac{\partial i_1}{\partial c_{H2O2}}\right)} * 100$$

where i_1 and i_2 are the cathodic currents for the electrode without and with rGO, respectively. For instance, for H_2O_2 concentration range from 10 to 100 µM, the increase in sensitivity ε = 185%, i.e. the sensitivity is almost three times higher for sensors with rGO.

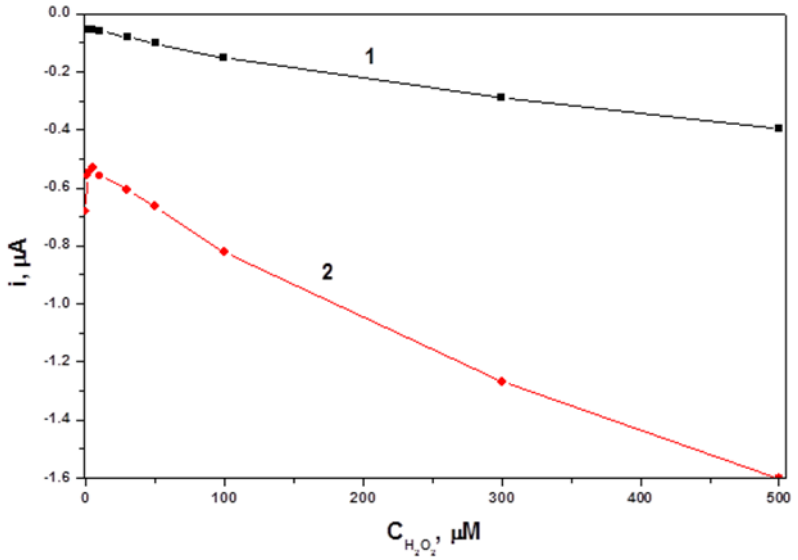

Figure 4. Dependence of the cathodic current of H_2O_2 reduction on C_{H2O2}, in 0.05 M potassium phosphate buffer with pH 6.00 containing 0.1M KCl, at E = 0 mV vs. Ag/AgCl, for: (1) bare spectroscopic graphite (SGE) and (2) SGE modified with a reduced graphene oxide (rGO).

Electrocatalytic effect of PB nanoparticles on H_2O_2 reduction

The deposition of PB nanoparticles was carried out using a solution containing 1.5 mM $K_3[Fe(CN)_6]$, 1.5 mM $FeCl_3$, 0.1 M KCl, and 3 mM HCl. Prussian Blue is formed during potential scanning and observed redox peaks increase with the number of cycles confirming the PB growth. Typical cyclic voltammetry (CV) characteristics obtained during film deposition on a bare SGE electrode and a rGO-modified electrode are presented in Figure 5.

This figure shows „potential shift“. Typical procedure for deposition of Prussian Blue onto graphite electrode uses potential scale from -0.2 V to 0.4 V vs. Ag/AgCl. But after modification by rGO, the "deposition peak" disappeared. This Figure shows that to deposit Prussian Blue onto rGO modified electrode, a wider potential window needs to be selected. In the case of the conditions of Figure 5, the upper potential limit has to be increased to 0.6 V vs. Ag/AgCl.

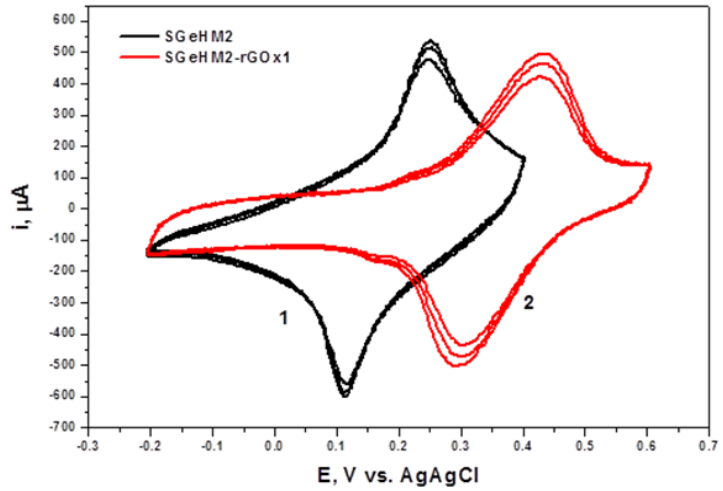

Figure 5. Deposition of Prussian Blue nanoparticles (PB) on: (1) bare SGE electrode and (2) SGE/rGO modified electrode, in 1.5 mM $K_3[Fe(CN)_6]$, 1.5 mM $FeCl_3$, 0.1 M KCl, and 3 mM HCl; scane rate v = 50 mV/s, electrode surface area: 0.19 cm^2.

Once a PB film is formed, it undergoes conversion between Prussian White (PW), which is the most reduced form, Prussian Blue (PB), and Berlin Green (BG), which is the most oxidized form. The electrode reactions associated with these conversions are presented below:

$$Fe(III)_4[Fe(II)(CN)_6]_3 + 4e^- + 4K^+ \leftrightarrows K_4Fe(II)_4[Fe(II)(CN)_6]_3 \quad (1)$$

PB PW

$$Fe(III)_4[Fe(II)(CN)_6]_3 + 3Cl^- \leftrightarrows Fe(III)_4[Fe(III)(CN)_6]_3Cl_3 + 3e^- \quad (2)$$

PB BG

The equilibrium potentials for these two processes on non-interacting surfaces are [47 57]: $E_{1,eq}$ = 0.197 V and $E_{2,eq}$ = 0.873 V vs. Ag/AgCl, respectively. In H_2O_2 sensors, the electron transfer of the conversion PB ↔ PW is utilized.

Several sensors and biosensors for the detection of H_2O_2 have been designed. The performance of a non-enzymatic rGO/PB-modified electrode in H_2O_2 solutions in the concentration range from 1 to 500 µM is presented in Figure 6.

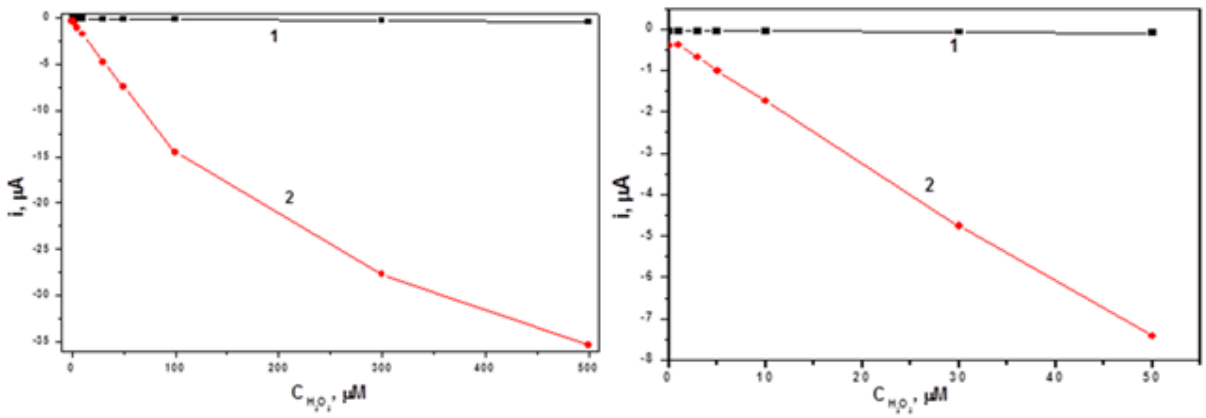

Figure 6. Dependence of H_2O_2 reduction current on H_2O_2 concentration for a spectroscopic graphite electrode: (1) bare SGE and (2) SGE modified with PB. Solutions: 50 mM PBS buffer + 100 mM KCl + x M H_2O_2, pH = 6.0.

The reduction currents are associated with the reduction of the analyte (H_2O_2). They are measured at the constant potential E = 0 V vs. Ag/AgCl reference. It is seen that the sensor performance is superb in comparison to the bare spectroscopic graphite electrode SGE and SGE/rGO sensor. It is clear that the electron mediation via Prussian Blue electrocatalyst nanoparticles is crucial for the sensor performance.

Effect of rGO on PB-catalyzed H_2O_2 reduction

The effect of rGO on PB-catalyzed H_2O_2 reduction is illustrated in Figure 7. This Figure shows that much better response in wider scale can be achieved using a combination of rGO and PB. Detailed examination of the performance graphs indicate that the background current for SGE/PB is lower (-0.4 µA) than that for SGE/rGO/PB (-1.6 µA). Therefore, the response of the sensor to H_2O_2 in the low concentration range (0 – 4 µM) is obscured in the presence of rGO. However, the addition of rGO enables maintaining high sensitivity of the sensor and its linear response to much higher H_2O_2 concentrations.

The roles of PB and rGO in improving the sensor performance can be evaluated by taking into account the initial slopes $(\partial i/\partial c)_{c=0}$ of characteristics in Figure 7 and the curve divergence at higher H_2O_2 concentrations. Since for both characteristics, the initial slopes are similar, it means that the PB presence plays the major role in the net electrocatalytic effect.

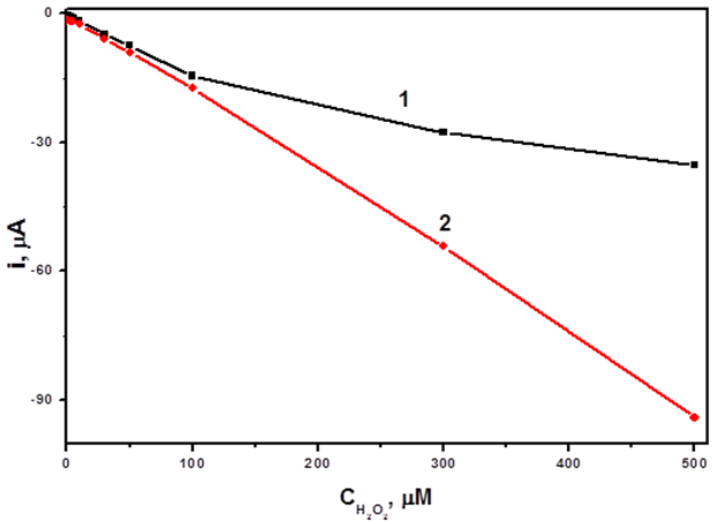

Figure 7. Dependence of H_2O_2 reduction current on H_2O_2 concentration for a modified spectroscopic graphite electrode: (1) SGE/PB and (2) SGE/rGO/PB. Solutions: 50 mM PBS buffer + 100 mM KCl + x M H_2O_2, pH = 6.0; E = 0 V vs. Ag/AgCl, surface 0.19 cm^2.

On the other hand, the curve divergence at higher H_2O_2 concentrations points to the benefit of high surface area and the necessity of minimizing the ohmic potential drop in the sensory film. Thus, the role of rGO is to efficiently distribute electrons from the bulk electrode to catalytically active surface centers and provide a large number of electron mediation centers on abundant PB nanoparticles. Also, it reduces the potential barrier that forms in low-conductance films[58], thus reducing the nonspecific electrolyte interference.

The fast charge delivery is corroborated by the short response time, τ_R = 5 s, which we have been able to achieve with SGE/rGO/PB sensors.

Graphene-based enzymatic biosensors for detection of phenols and polyphenols

Enzyme biosensors commonly utilize the electrochemical transduction paradigm to quantitate a bioanalyte via the electrochemical detection of H_2O_2 that is generated as a

byproduct in the reaction of bioanalyte species with the enzyme molecules immobilized in the sensory film of a biosensor. Here, for the sake of comparison and to assess the performance of electrocatalytic sensors, we present the reactivities of two kinds of the third–generation biosensors based on graphene (rGO): one with horseradish peroxidase (HRP) and one with laccase oxidase (LACC) anchored in the sensory films.

In Figure 8, the electrochemical response of a SGE/rGO/PB sensor, with immobilized HRP, to catechin concentration is presented and compared to the same electrode in which HRP has been replaced with BSA. Here H_2O_2 is added as the reaction substrate.

The operation of this SGE/rGO/PB/HRP sensor for catechin is based on the principle that HRP enzyme molecules first reduce hydrogen peroxide present in the solution and become oxidized. In this state, they can oxidize catechin molecules converting them to quinones or free radicals. The latter products are electroactive and can react on the electrode surface at convenient potentials close to 0 V vs. Ag/AgCl. While we were not able to discern products of this reaction, we can clearly see lowering of the cathodic current of the reduction of hydrogen peroxide substrate. The reduction current lowering is directly proportional to the concentration of catechin in solution.

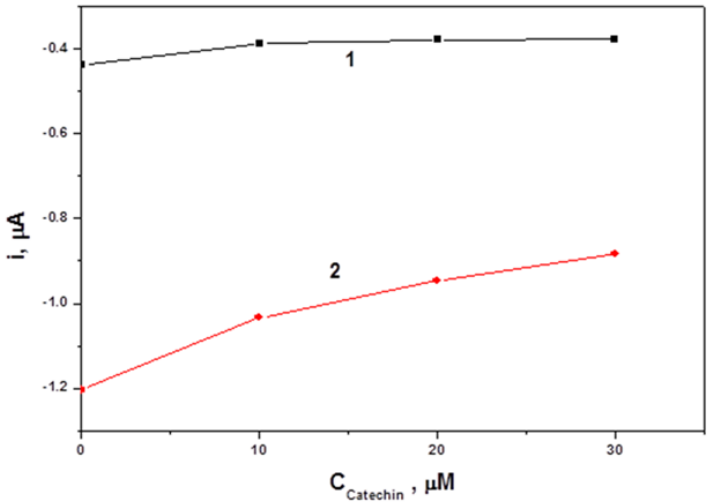

Figure 8. Dependence of the biosensor reduction current on catechin concentration $c_{catechin}$ for a modified SGE/rGO/PB graphite electrode with immobilized: (1) BSA and (2) HRP. Solutions: 50 mM PBS buffer + 100 mM KCl + 1 mM H_2O_2, pH = 6.0; E = 0 V vs. Ag/AgCl, surface 0.19 cm^2.

In Figure 9, the electrochemical response of a SGE/rGO/PB sensor, with immobilized LACC enzyme, to catechin concentration is presented and compared to the same electrode in which LACC has been replaced with BSA. In contrast to the HRP-containing biosensor, H_2O_2 is not used here as the reaction substrate.

The operation of the SGE/rGO/PB/LACC biosensor for catechin is based on the fact that catechin, similar to other polyphenols, can act as the electron donor. Thus, LACC oxidizes catechin with parallel reduction of oxygen molecules to water. The LACC enzyme catalyzes removal of a hydrogen atom from the hydroxylic group of ortho- and para-subsituted mono- and polyphenolic substrates. As seen in Figure 9, the cathodic current increases with increasing catechin concentration.

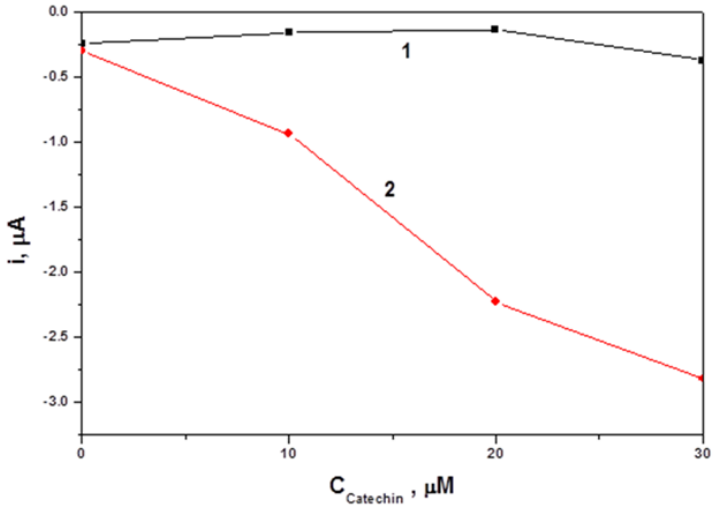

Figure 9. Dependence of the biosensor reduction current on catechin concentration $c_{catechin}$ for a modified SGE/rGO/PB graphite electrode with immobilized: (1) BSA and (2) LACC. Solutions: 50 mM PBS buffer + 100 mM KCl, pH = 6.0; E = 0 V vs. Ag/AgCl, surface 0.19 cm^2.

These experiments demonstrate that the high catalytic activity of rGO-supported "artificial enzyme" PB can be utilized in designing biosensors based on detecting H_2O_2 and related species. The employed enzyme activity (15 U/cm^2) is consistent with our previous studies[32-34] on enzymatic biosensors for polyphenols and other analytes but it can be further optimized for a particular application. Note that the proposed sensors have been designed to operate at a low current density in order to minimize the analyte depletion in the vicinity of the electrode surface. For this reason, the potential has been selected at the foot of the voltammetric wave, at E = 0 V vs. Ag/AgCl (see: Figure 3). By applying a lower potential, e.g. at the peak potential (E_p = -0.3 V) or lower, and using cyclic voltammetry or pulse measurements, the signal recorded can be increased considerably if desired. Future investigations will be directed toward miniaturization feasibility of the rGO/PB sesnsing platform.

Conclusions

We have developed a facile and inexpensive method for designing high performance sensors for H_2O_2 and polyphenols. The proposed sensors are based on high electrocatalytic activity of Prussian Blue (PB) nanoparticles electrodeposited on a film of exfoliated graphene nanosheets on a graphite electrode (SGE). The graphene nanosheets were obtained by casting a graphene oxide film on SGE, followed by its electrochemical reduction to obtain the reduced graphene oxide (rGO). The PB catalyst nanoparticles were grown electrochemically on rGO. This proposed procedure is very time efficient as it reduces the time of sensor preparation from 3 days (according to recent literature) to several hours. The sensors exhibit a linear response range from 1 to 500 μM H_2O_2 and response time of 5 s. Furthermore, we have demonstrated that these sensors can be combined with immobilized enzymes (horseradish peroxidase or laccase oxidase), to serve as biosensors for the determination of polyphenols. As an example, biosensors with immobilized horseradish peroxidase or laccase oxidase have been constructed and tested with a polyphenol catechin. The proposed sensors are low cost, reliable, and scalable.

Acknowledgements

Funding for this project was provided through NSF CCLI grant No. 0941364. O. Kubesa is grateful for support from the INBIOR project (CZ.1.07/2.3.00/20.0042).

References

1- K.S. Novoselov, A.K. Geim, S.V. Morozov, D. Jiang, Y. Zhang, S.V. Dubonos, I.V. Grigoreva and A.A. Firsov, *Science*, **2004**, 306, 666-669.
2- A.K. Geim and K.S. Novoselov, *Nature Mater.*, **2007**, 6, 183-191.
3- M. Pumera, A. Ambrosi, A. Bonanni, E.L.K. Chng and H.L. Poh, *Trends Anal. Chem.*, **2010**, 29, 954-965.
4- M. Hepel, in *Encyclopedia of Surface and Colloid Science*; ed. P. Somasundaran; Taylor and Francis: New York, 2014, pp. 1-15 (in press).
5- C.M. Chen, Q.H. Yang, Y.G. Yang, W. Lv, Y.F. Wen, P.X. Hou, M.Z. Wang and H.M. Cheng, *Adv. Mater.*, **2009**, 21, 3007-3011.
6- H.Q. Chen, M.B. Muller, K.J. Gilmore, G.G. Wallace and D.Li, *Adv. Mater.*, **2008**, 20, 3557-3561.
7- J.J. Liu, X.L. Zhang, Z.X. Cong, Z.T. Chen, H.H. Yang and G.N. Chen, *Nanoscale*, **2013**, 5, 1810-1815.
8- Y. Wang, Y.M. Li and L.H. Tang, *Electrochem. Commun.*, **2009**, 11, 889-892.
9- L. Tan, K.G. Zhou, Y.H. Zhang and e. al., *Electrochem. Commun.*, **2010**, 12, 557-560.
10- X.P. Chen, H.Z. Ye and W.Z. Wang, *Electroanalysis*, **2010**, 20, 2347-2352.
11- P. Wu, S.A. Qian and Y.J. Hua, *Electrochim Acta*, **2010**, 55, 8606-8614.
12- J.W. Wang, S.L. Yang, D.Y. Guo, P. Yu, D. Li, J.S. Ye and L.Q. Mao, *Electrochem. Commun.*, **2009**, 11, 1892-1895.
13- W.J. Lin, C.S. Liao, J.H. Jhang and Y.C. Tsai, *Electrochem. Commun.*, **2009**, 11, 2153-2156.
14- B. Hong and Q. Cheng, *Adv. Chem. Engng. Sci.*, **2012**, 2, 453-460.
15- J.T. Robinson, F.K. Perkins, E.S. Snow, Z. Wei and P.E. Sheehan, *Nano Lett.*, **2008**, 8, 3137-3140.
16- H. Gong, M. Sun, R. Fan and L. Qian, *Microchim. Acta*, **2013**, 180, 295-301.
17- X.W. Liu, Z.J. Yao, Y.F. Wang and X.W. Wei, *Colloids Surf. B*, **2010**, 81, 508-512.
18- Y. Zhang, X.M. Sun, L.Z. Zhu, H.B. Shen and N.Q. Jia, *Electrochim. Acta*, **2011**, 56, 1239-1245.
19- D. Li, M.B. Muller, S. Gilje, R.B. Kaner and G.G. Wallace, *Nat. Nanotechnol.*, **2008**, 3, 101-105.
20- K. Mikhoyan, A. Contryman, J. Silcox, D. Steward, G. Eda, C. Mattevi, S. Miller and M. Chhowalla, *Nano Lett.*, **2009**, 9, 1058-1063.
21- D. Kosynkin, A. Higginbotham, A. Sinitskii, J. Lomeda, A. Dimiev, K. Price and J. Tour, *Nature*, **2009**, 458, 872-876.
22- G. Eda, G. Fanchini and M. Chhowalla, *Nat. Nanotechnol.*, **2008**, 3, 270-274.
23- S. Stankovich, D.A. Dikin, R.D. Piner, K.A. Kohlhaas, A. Kleinhammes, Y. Jia, Y. Wu, S.T. Nguyen and R.S. Ruoff, *Carbon*, **2007**, 45, 1558-1565.
24- N.A. Kotov, I. Dekany and J.H. Fendler, *Adv. Mater.*, **1996**, 8, 637-641.
25- D. Yang, A. Velamakanni, G. Bezoklu, S. Park, M. Stoller, R.D. Piner, S. Stankovich, I. Junk, D.A. Field, C.A. Ventrice and R.S. Ruoff, *Carbon*, **2009**, 47, 145-152.

26- Y. Si and E.T. Samulski, *Nano Lett.*, **2008**, 8, 1679-1682.
27- H.J. Shin, K.K. Kim and A. Benayad, *Adv. Functional Materials*, **2009**, 19, 1987-1992.
28- G.K. Ramesha and S. Sampath, *J. Phys. Chem. C*, **2009**, 113, 7985-7989.
29- Z. Wang, X. Zhou and J. Zhang, *J. Phys. Chem. Lett.*, **2009**, 113, 14071-14075.
30- E. Jin, X.F. Lu, L.L. Cui, D.M. Chao and C. Wang, *Electrochim. Acta*, **2010**, 55, 7230-7234.
31- M. Hepel, M. Stobiecka, J. Peachey and J. Miller, *Mutation Res.*, **2012**, 735, 1-11.
32- R. Solna and P. Skladal, *Electroanalysis*, **2005**, 17, 2137-2146.
33- J. Zeravik, K. Lacina, M. Jilek, J. Vlcek and P. Skladal, *Microchim. Acta*, **2010**, 170, 251-256.
34- J. Zeravik, A. Hlavacek, K. Lacina and P. Skladal, *Electroanalysis*, **2009**, 21, 2509-2520.
35- K. Itaya, N. Shoji and I. Uchida, *J. Am. Chem. Soc.*, **1984**, 106, 3423-3429.
36- A.A. Karyakin, E.E. Karyakina and L. Gorton, *J. Electroanal. Chem.*, **1998**, 456, 97-104.
37- A.A. Karyakin, O.V. Gitelmacher and E.E. Karyakina, *Anal. Chem.*, **1995**, 67, 2419-2423.
38- S.A. Jaffari and A.P.F. Turner, *Biosens. Bioelectron.*, **1997**, 12, 1-9.
39- F. Ricci, A. Amine, G. Palleschi and D. Moscone, *Biosens. Bioelectron.*, **2003**, 18, 165-174.
40- J.D. Qiu, H.Z. Peng, R.P. Liang, J. Li and X.H. Xia, *Langmuir*, **2007**, 23, 2133-2137.
41- Z. Chu, Y. Zhang, X. Dong, W. Jin, N. Xu and B. Tieke, *J. Mater. Chem.*, **2010**, 20, 7815–7820.
42- C. Lete, S. Lupu, M. Marin and M. Badea, *Rev. Roum. Chim.*,, **2010**, 55, 335-340.
43- P. Salazar, M. Martín and R. Roche, *Electrochim. Acta*, **2010**, 55, 6476-6484.
44- A.L. Sanford, S.W. Morton, K.L. Whitehouse, H.M. Oara, L.Z. Lugo-Morales, J.G. Roberts and L.A. Sombers, *Anal. Chem.*, **2010**, 82, 5205-5210.
45- J.D. Qiu, M. Xiong, R.P. Liang, J. Zhang and X.H. Xia, *J. Nanosci. Nanotechnol.*, **2008**, 8, 4453-4460.
46- L.Y. Cao, Y.L. Liu, B.H. Zhang and L.H. Lu, *ACS Appl. Mater. Interfaces*, **2010**, 2, 2339-2346.
47- Y.Y. Jiang, X.D. Zhang, C.S. Shan, S.H. Hua, X.Q. Zhang, X.X. Bai, L. Dan and L. Niu, *Talanta*, **2011**, 85, 76-81.
48- M.T. Sulak, E. Erhan, B. Keskinler, F. Yılmaz and A. Celik, *Sensor Lett.*, **2010**, 8, 262-267.
49- M.T. Sulak, E. Erhan and B. Keskinler, *Sensors Materials*, **2012**, 24, 141-152.
50- J.A. Rather and K.D. Wael, *Sensors Actuators B*, **2012**, 171-172, 907-915.
51- J.A. Rather and K.D. Wael, *Sensors Actuators B*, **2013**, 176, 110-117.
52- J.A. Rather, P. Debnath and K.D. Wael, *Electroanalysis*, **2013**, 25, 2145-2150.
53- A. Qurashi, J.A. Rather, K.D. Wael, B. Merzougui, N. Tabet and M. Faiz, *Analyst*, **2013**, 138, 4764-4768.
54- J.A. Rather, S. Pilehvar and K.D. Wael, *Sensors Actuators B*, **2014**, 190, 612-620.
55- W.S. Hummers and R.E. Offeman, *J. Am. Chem. Soc.*, **1958**, 80, 1339-1339.
56- D.C. Marcano, D.V. Kosynkin, J.M. Berlin, A. Sinitskii, Z. Sun, A. Slesarev, L.B. Alemany, W. Lu and J.M. Tour, *ACS Nano*, **2010**, 4, 4806-4814.
57- A.A. Karyakin, *Electroanalysis*, **2001**, 13, 813–819.
58- M. Stobiecka and M. Hepel, *Biosens. Bioelectron.*, **2011**, 26, 3524-3530